

# Search for Chemisorbed HCO: The Interaction of Formaldehyde, Glyoxal, and Atomic Hydrogen + CO with Rh

J. T. YATES, JR.<sup>1</sup> AND R. R. CAVANAGH<sup>2</sup>

*Surface Science Division, National Bureau of Standards, Washington, D.C. 20234*

Received May 13, 1981; revised September 14, 1981

Transmission infrared spectroscopy has been used to search for the chemisorptive stabilization of formyl (HCO) on Al<sub>2</sub>O<sub>3</sub>-supported Rh surfaces. Formaldehyde (H<sub>2</sub>CO) and glyoxal (HCO)<sub>2</sub> have been used as potential sources of HCO. In addition, chemisorbed CO on Rh has been treated with atomic deuterium in an attempt to produce DCO. None of these routes have led to spectroscopically detectable levels of formyl adsorption at temperatures near or above 100 K. These results suggest that the formyl intermediate may not be a stable surface species on Rh in CO-hydrogenation chemistry.

## I. INTRODUCTION

Mechanistic details of the catalytic production of CH<sub>4</sub> and larger hydrocarbons from H<sub>2</sub>(g) + CO(g) have been the subject of much recent speculation. Experimental studies in coupled high-pressure/ultrahigh-vacuum systems have demonstrated the active role of surface carbon (or CH<sub>x</sub> species) on Ni single crystals in such reactions (1). The capacity to form CH<sub>4</sub> from the reaction with H<sub>2</sub>(g) of CO-produced surface carbon indicates that CO dissociation is a compatible first step in the catalytic reaction pathway to CH<sub>4</sub>. Further studies of various types have supported the CO dissociation mechanism on Ru (2-4). Similar conclusions have been reached regarding C formation from CO on polycrystalline Rh surfaces (5), and in particular on stepped Rh single crystals (6, 7), although the efficiency of CO dissociation processes on Rh is a controversial issue at present (7).

Contrary to a model involving dissociative CO chemisorption as the primary ele-

mentary step in the catalytic formation of hydrocarbons, mechanisms involving the hydrogenation of CO to form various intermediates such as HCO(ads) or HCOH(ads) have also been widely discussed in the recent literature, as exemplified in a review article by Muetterties and Stein (8), as well as in earlier reviews (9). In addition, experimental observations which detected small quantities of CH<sub>4</sub> produced from H<sub>2</sub>CO chemisorption on Ru(110) (10) and on W(100) and W(111) (11, 12) have lent support to the alternate model, in which species like adsorbed formyl, HCO(ads), are postulated to be involved in the catalytic synthesis of CH<sub>4</sub> from CO and H<sub>2</sub>. While the exact role played by these species during a chemical reaction is not known, the synthesis of model inorganic compounds containing such functional groups clearly demonstrates their existence (13).

The work to be discussed in this paper addresses the question of the stabilization of species like HCO(ads) on an Al<sub>2</sub>O<sub>3</sub>-supported Rh surface. We have employed molecules such as H<sub>2</sub>CO and (HCO)<sub>2</sub> as adsorbates at 100 K. Transmission infrared spectroscopy was used to search for intermediates in the catalytic decomposition of these molecules as the surface was warmed to 340 K. In addition, atomic deuterium was employed as a reactant with chemi-

<sup>1</sup> Present address: Department of Chemistry, University of Pittsburgh, Pittsburgh, Pa. 15260.

<sup>2</sup> NRC-NBS Postdoctoral Research Associate 1979-1981. Present address: Molecular Spectroscopy Division, National Bureau of Standards, Washington, DC 20234.

sorbed CO on Rh in an attempt to produce DCO(ads).

The combination of low-temperature adsorption techniques with infrared spectroscopy on supported metal systems is a potentially promising method for trapping and observing such transient reaction intermediates. Temperature-dependent surface binding state distributions between 77 and 300 K are well known on single-crystal substrates from investigations using a variety of surface-sensitive spectroscopies, yet rarely have such species been studied using the infrared transmission technique. The combination of low-temperature methods with model adsorbate systems provides a unique opportunity to prepare, isolate, and study various proposed reaction intermediates.

## II. EXPERIMENTAL

Complete details of the sample preparation, vacuum system, and spectrometer have appeared elsewhere (14, 15). In brief, a solution of Rh<sup>III</sup> ions was prepared by dissolving RhCl<sub>3</sub> · 3H<sub>2</sub>O in water. This mixture was then used to impregnate an amount of Al<sub>2</sub>O<sub>3</sub> (DeGussa-C)<sup>3</sup> such that the weight percentage of rhodium would be 2.2%. Acetone was then added to the solution (10:1 = acetone:water). This slurry was sprayed onto a CaF<sub>2</sub> plate held at 350 K causing flash evaporation of solvents. Typical deposit loadings of 11 mg/cm<sup>2</sup> were obtained. The deposited sample was then mounted in the ultrahigh-vacuum infrared cell, outgassed at 425 K, reduced in H<sub>2</sub> at 425 K, and further outgassed at 475 K for 8 h. This Rh preparation adsorbs 1.2 CO molecules per Rh atom and exhibits a specific surface area of 55 m<sup>2</sup>/g as measured by N<sub>2</sub>-BET procedures (14, 18). All infrared spectra were recorded on a Perkin-Elmer model 180 infrared spectrometer.<sup>3</sup>

H<sub>2</sub>CO(g) was prepared by heating para-

formaldehyde in a gas generator at 350 K, passing the gas through a glass trap at 195 K, and directly admitting the H<sub>2</sub>CO(g) to the stainless-steel manifold. The purity of the H<sub>2</sub>CO(g) obtained by this method is well established (11).

(CHO)<sub>2</sub>(g) was obtained using established literature methods (16). A mixture of P<sub>2</sub>O<sub>5</sub> and trimeric glyoxal dihydrate (C<sub>2</sub>H<sub>2</sub>O<sub>2</sub>)<sub>3</sub> · (2H<sub>2</sub>O) (1:1) was placed in a glass system similar to that used for the formaldehyde generator. The generator was evacuated and the glass trap immersed in liquid nitrogen. While pumping on the generator/trap, the mixture was gently heated. In addition to the evolution of noncondensable gases, both yellow crystals and white crystals appeared in the glass trap. The P<sub>2</sub>O<sub>5</sub>/(C<sub>2</sub>H<sub>2</sub>O<sub>2</sub>)<sub>3</sub> · (2H<sub>2</sub>O) vessel was isolated from the trap, and the trap was brought to 195 K, at which time the evolution of additional noncondensables and the disappearance of the white crystals were noted. The remaining yellow crystals were further purified by a freeze-pump-thaw cycle. The pressure of an aliquot of vapor obtained from this purified sample upon warming was found to be stable in the stainless-steel manifold to 0.1% over several minutes.

The generation of deuterium atoms was achieved with a thermal source operating in a D<sub>2</sub> atmosphere. In these experiments, a high-temperature tungsten filament was operated inside the infrared cell (see Fig. 1). The adsorbent was shielded from radiation from the filament by means of a baffle arrangement. The D<sub>2</sub> gas-phase pressure in the range 0.2–0.01 Torr was monitored with a capacitance manometer as a function of filament temperature; we observed the initiation of a continuous pressure drop at the onset of D atom generation. This is presumably due to interaction of D atoms with the cell walls or the sample.

Due to the location of the thermocouple on the copper sample holder rather than within the sample itself, there is some uncertainty as to the exact temperature of the

<sup>3</sup> The identification of specific suppliers and manufacturers is provided to aid the reader. No endorsement of this product by NBS is implied.

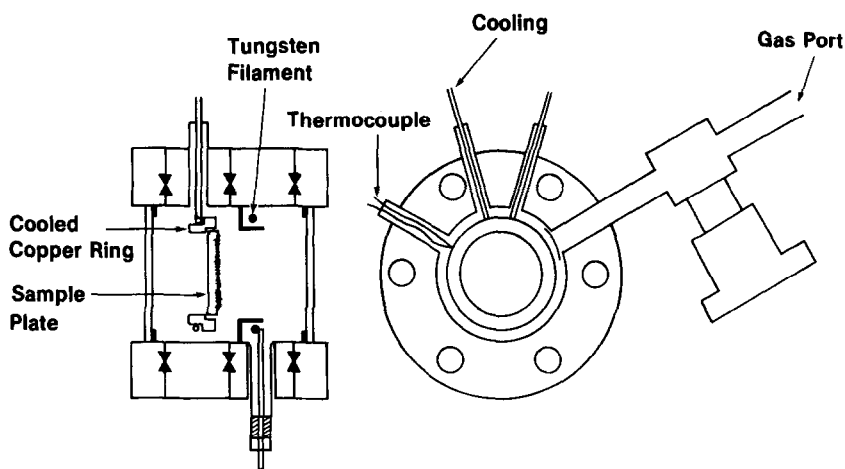


FIG. 1. Variable-temperature infrared cell. The tungsten filament for dissociation of  $D_2$  to atomic D is indicated, behind the L-shaped radiation shield.

specimen. Rather than attempt to correct for this error, the temperatures given refer simply to the temperature of the copper support assembly. Preferential condensation of  $H_2CO$  and  $(HCO)_2$  on the copper sample holder is observed at  $T \leq 100$  K.

### III. INTERACTION OF FORMALDEHYDE WITH $Al_2O_3$ AND WITH $Rh/Al_2O_3$ —RESULTS

#### A. $H_2CO$ Adsorbed on $Al_2O_3$

A Rh-free sample of  $Al_2O_3$  weighing 58 mg was prepared as described under Experimental. This sample was then cooled to  $\sim 100$  K and exposed to  $6 \times 10^{19}$  molecules of  $H_2CO(g)$ . This dose of  $H_2CO$  corresponded to  $\sim 1$  molecule per  $10 \text{ \AA}^2$  of  $Al_2O_3$  surface area. Following measurement of the infrared spectrum, the surface was warmed in a stepwise fashion to 300 K and spectral developments were followed, as shown in Fig. 2. Finally, at 300 K, the cell was evacuated and spectrum 2e was recorded.

At 160 K, a distinct feature due to physisorbed  $H_2CO$  develops near  $1700 \text{ cm}^{-1}$ ; upon warming the dosed cell to 300 K, the  $1700\text{-cm}^{-1}$  feature has diminished in intensity, while additional absorbance due to  $H_2CO(g)$  develops near  $1750 \text{ cm}^{-1}$ . After evacuation at 300 K, there is little evidence

for either feature. However, new features which appear at  $1591$ ,  $1392$ , and  $1372 \text{ cm}^{-1}$  persist upon evacuation. These three features are in excellent agreement with those reported for formate production from  $CH_3OH$  decomposition on  $Al_2O_3$  [ $1597$ ,  $1394$ ,  $1377 \text{ cm}^{-1}$ ] (17).

The region between  $2700$  and  $2000 \text{ cm}^{-1}$  was carefully examined during this experiment, since this is the region in which the H-C stretching frequency for  $HCO(ads)$  would be expected. The only additional feature which appeared was a broad weak feature near  $2040 \text{ cm}^{-1}$  (6% of the  $1700\text{-cm}^{-1}$  peak intensity). This feature disappears upon evacuation at 300 K. Table 1 summarizes the observed spectral features in this series of measurements.

#### B. $H_2CO$ Adsorbed on $Rh/Al_2O_3$

A 61-mg sample containing 2.2% Rh was prepared. Following cooling to 100 K, the sample was exposed to  $8 \times 10^{18}$  molecules of  $H_2CO(g)$ . From previous experiments we know that the chemisorptive capacity of this  $Rh/Al_2O_3$  sample for  $CO(g)$  should be  $\sim 1.1 \times 10^{19}$  CO molecules (18).

The spectral development as a function of temperature is shown in Fig. 3. The spectral feature observed near  $1700 \text{ cm}^{-1}$  at 160

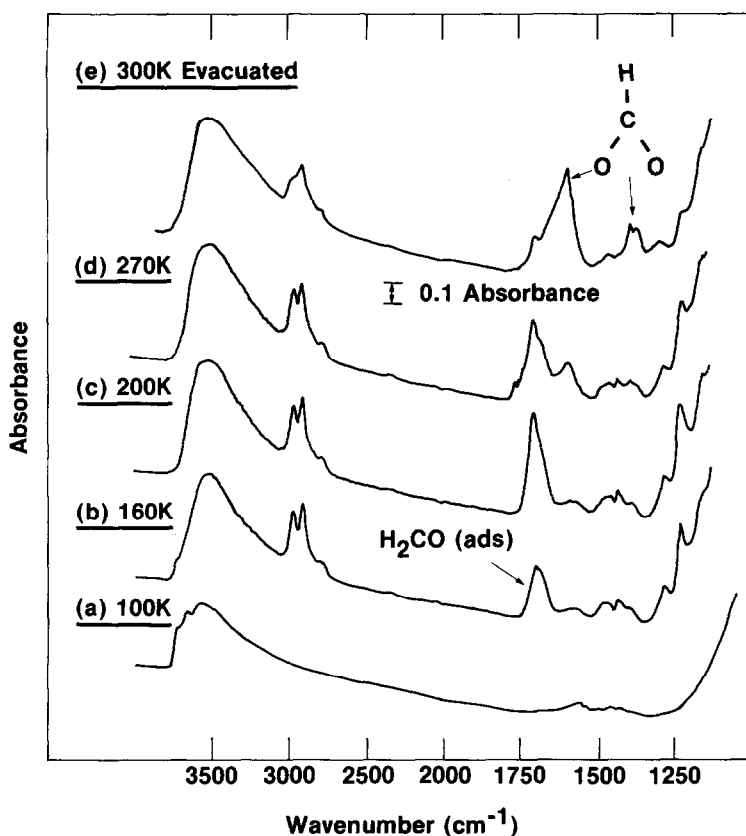


FIG. 2. Infrared spectrum of  $\text{H}_2\text{CO}$  adsorbed on  $\text{Al}_2\text{O}_3$ . The sample is dosed with formaldehyde while at 100 K (a). Spectra b–d indicate changes while warming to the indicated temperature. Spectrum e was recorded after evacuating the sample to  $\sim 1 \times 10^{-3}$  Torr.

K can be associated with  $\text{H}_2\text{CO}$  physisorbed on  $\text{Al}_2\text{O}_3$ , as seen for pure  $\text{Al}_2\text{O}_3$  in Fig. 2. As the  $\text{Rh}/\text{Al}_2\text{O}_3$  sample is warmed, the development of additional spectral features between 2100 and 1800  $\text{cm}^{-1}$  is apparent. At 230 K spectral features at 1860, 2021, 2045, and 2088  $\text{cm}^{-1}$  are observed as well as H–C stretching modes at  $\sim 2910$  and  $\sim 2980$   $\text{cm}^{-1}$ . An additional weak feature at  $\sim 2790$   $\text{cm}^{-1}$  is also observed.

Previous work has shown that the 1860- $\text{cm}^{-1}$  feature can be assigned to bridge-bonded CO (14, 19, 20) on Rh crystallite sites. For pure CO adsorption, features in the region 2000–2100  $\text{cm}^{-1}$  have been assigned to terminal CO species on Rh crystallites [ $\sim 2050$ – $2070$   $\text{cm}^{-1}$ ] (14) and to  $\text{Rh}(\text{CO})_2$  species produced on isolated Rh

sites [2101 and 2031  $\text{cm}^{-1}$ ] (14, 18). The features at 2088 and 2021  $\text{cm}^{-1}$ , as produced by  $\text{H}_2\text{CO}(\text{g})$  adsorption, are  $\sim 10$   $\text{cm}^{-1}$  lower in wavenumber than the corresponding features produced by  $\text{CO}(\text{g})$  adsorption, in agreement with earlier observations for  $\text{H}_2\text{CO}$  adsorption on  $\text{Rh}/\text{Al}_2\text{O}_3$  (21). This 10- $\text{cm}^{-1}$  shift will be discussed in Section III.C.

It should be noted here that the intensity of absorbance in the region 2100 to 1800  $\text{cm}^{-1}$  for all of these features derived from  $\text{H}_2\text{CO}(\text{g})$  adsorption is much lower than expected for full CO coverage. This observation is confirmed also from the experiment shown in spectrum 3d where the  $\text{H}_2\text{CO}(\text{g})$  was pumped from the cell and  $^{12}\text{CO}(\text{g})$  was introduced. The significant increase in ab-

TABLE 1  
Infrared Features Observed for H<sub>2</sub>CO Adsorption on Al<sub>2</sub>O<sub>3</sub> (cm<sup>-1</sup>)

Sample temperature (K)		
<200	200-300	>300 + evacuation
2977	2977	2962
2913	2913	2908
2788	2788	2788
2040 (br)		
1700	1770-1700	1770-1700
	1594	1594
	1392	1392
	1372	1372
1470	1470	1470
1430	1430	
1395	1395	Unresolved
1280	1280	1300
1230	1230	1230
1150	1150	1150

sorbance at 1860, 2020, 2050, and 2093 cm<sup>-1</sup> indicates the presence of active Rh sites for CO chemisorption in spite of the high dose of H<sub>2</sub>CO(g).

*C. Perturbation of Rh-Chemisorbed CO Species by Adsorbates on the Al<sub>2</sub>O<sub>3</sub> Support*

It is possible that small spectral shifts for chemisorbed CO on Al<sub>2</sub>O<sub>3</sub>-supported Rh could be due to interactions with adsorbed CO caused by adsorption of other molecules on the Al<sub>2</sub>O<sub>3</sub> support, in much the same fashion as observed in matrix isolation infrared spectroscopy for changes in the matrix. Two experiments were carried out in order to check this point:

1. H<sub>2</sub>O + CO/Rh/Al<sub>2</sub>O<sub>3</sub>. A Rh/Al<sub>2</sub>O<sub>3</sub> sample was exposed to H<sub>2</sub>O(g) at 0.5 Torr pressure. Increased absorbance was observed in the OH stretching region between 3700 and 3000 cm<sup>-1</sup> and a feature due to H<sub>2</sub>O adsorption on Al<sub>2</sub>O<sub>3</sub> is observed in the HOH bending region near 1620 cm<sup>-1</sup>. Only

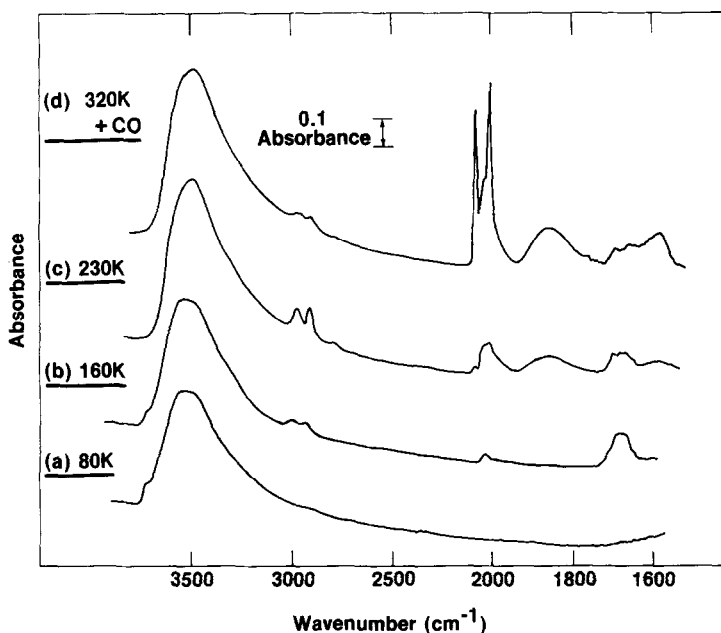


FIG. 3. Infrared spectrum of H<sub>2</sub>CO chemisorbed on Rh/Al<sub>2</sub>O<sub>3</sub>. a-c correspond to the spectral developments following introduction of H<sub>2</sub>CO at 80 K. Subsequent evacuation and saturation with CO resulted in spectrum d.

minor changes in CO-derived spectral features on Rh were observed when the evacuated sample was subsequently exposed to CO(g); spectral features at 2098, 2053, 2027, and 1860  $\text{cm}^{-1}$  were produced. This corresponds to an approximately 2- to 3- $\text{cm}^{-1}$  decrease in wavenumber for the doublet from values of 2101 and 2031  $\text{cm}^{-1}$  observed on  $\text{H}_2\text{O}$ -free surfaces.

2.  $\text{H}_2\text{CO} + \text{CO}/\text{Rh}/\text{Al}_2\text{O}_3$ . In a separate experiment, a 2.2% Rh sample was saturated with  $^{13}\text{CO}$  and evacuated (see Fig. 4) resulting in  $^{13}\text{CO}$  features at 2053, 2035, 1987, and 1825  $\text{cm}^{-1}$ . This sample was subsequently exposed to a saturation coverage of  $\text{H}_2^{12}\text{CO}$  [see Fig. 4c]. The features previously associated with the formation of formates on the  $\text{Al}_2\text{O}_3$  are clearly present. In addition, the two sharp ir peaks associated with  $^{13}\text{CO}$  bound to Rh as  $\text{Rh}(\text{CO})_2$  were observed to shift to lower wavenumber by 10  $\text{cm}^{-1}$  to 2042 and 1975  $\text{cm}^{-1}$ . Introduction of additional  $\text{H}_2\text{CO}$  resulted in a further shift of the  $^{13}\text{CO}$  features. The significant shift in the  $^{13}\text{CO}$  features and the absence of infrared evidence for  $^{12}\text{CO}$ -

$^{13}\text{CO}$  exchange demonstrate a strong support perturbation of the Rh-bound CO modes attributable to the presence of oxide-bound species derived from  $\text{H}_2\text{CO}$ . A similar  $\text{H}_2\text{CO}$ -induced shift has been seen for  $^{13}\text{CO}$  on Rh at 300 K (21).

#### IV. INTERACTION OF GLYOXAL WITH $\text{Al}_2\text{O}_3$ AND WITH $\text{Rh}/\text{Al}_2\text{O}_3$ —RESULTS

##### A. $(\text{HCO})_2$ Adsorbed on $\text{Al}_2\text{O}_3$

In Fig. 5, a 55-mg sample of  $\text{Al}_2\text{O}_3$  was exposed to  $4 \times 10^{19}$   $(\text{HCO})_2(\text{g})$  molecules at 100 K and then warmed. Infrared spectra as a function of sample temperature are shown. Spectrum 5a indicates the presence of very little adsorbate on the  $\text{Al}_2\text{O}_3$ , presumably because of condensation of the  $(\text{HCO})_2(\text{g})$  on cooler regions of the sample support assembly. Upon warming to 190 K, two predominant peaks at 1720 and 1748  $\text{cm}^{-1}$  are observed as  $(\text{HCO})_2$  transfers to the  $\text{Al}_2\text{O}_3$ . Between 235 and 275 K, an inversion of relative intensity occurs as the intensity of the 1720- $\text{cm}^{-1}$  feature decreases while the intensity of the 1748- $\text{cm}^{-1}$  fea-

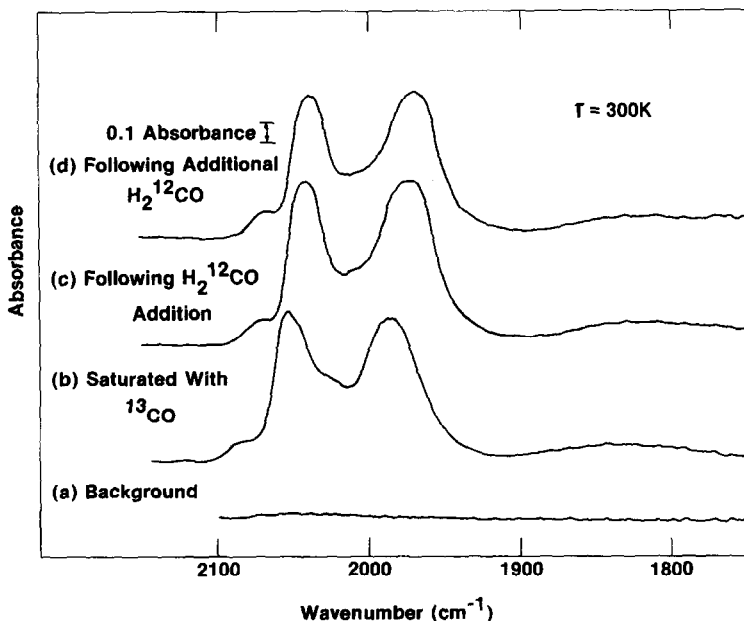


FIG. 4. Perturbation of  $^{13}\text{CO}(\text{ads})$  on  $\text{Rh}/\text{Al}_2\text{O}_3$  following exposure to  $\text{H}_2^{12}\text{CO}(\text{g})$ .

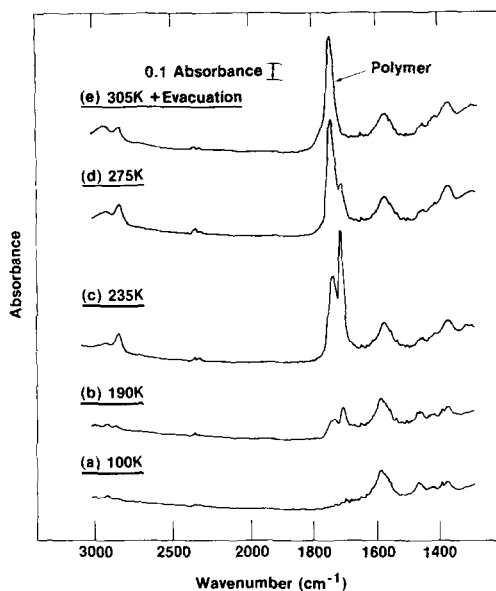


FIG. 5. Infrared spectrum of glyoxal (HCO)<sub>2</sub> adsorbed on Al<sub>2</sub>O<sub>3</sub>.

ture increases. The only other features observed between 3200 and 1400 cm<sup>-1</sup> were bands at 2930 and 2840 cm<sup>-1</sup>. There are small changes in the relative intensity of these two bands during sample warming, but both bands persist upon evacuation of the cell. The behavior observed on warming the Al<sub>2</sub>O<sub>3</sub> surface from 190 to 305 K is not observed to be reversible upon subsequent cooling back to 100 K. The presence of an intense feature at 1748 cm<sup>-1</sup> upon evacuation at 305 K is in distinct contrast to the behavior observed for H<sub>2</sub>CO on Al<sub>2</sub>O<sub>3</sub> (Fig. 2), where irreversibly adsorbed formate species are produced.

### B. (HCO)<sub>2</sub> Adsorbed on Rh/Al<sub>2</sub>O<sub>3</sub>

The adsorption of (HCO)<sub>2</sub>(g) on a 2.3% Rh sample weighing 90 mg is shown in Fig. 6. By comparison with data obtained for pure Al<sub>2</sub>O<sub>3</sub> (Fig. 5) it may be seen that the behavior in the region 1700–1800 cm<sup>-1</sup> and in the region 2800–3000 cm<sup>-1</sup> is very similar, suggesting that these spectral features are unrelated to the interaction of (HCO)<sub>2</sub>

with Rh. At temperatures above 190 K, new infrared features in the region 1800–2100 cm<sup>-1</sup> are observed due to the interaction of (HCO)<sub>2</sub> with Rh. Comparison of glyoxal spectrum 5c with formaldehyde spectrum 3c suggests that the infrared spectra of the species present on the Rh sites are very similar although relative intensities differ somewhat. Thus in each case we observe major bands at ~2045 and ~1860 cm<sup>-1</sup> similar to those observed for low coverages of CO(ads) on crystalline Rh sites (14, 18). In addition small features at ~2090 and ~2020 cm<sup>-1</sup> are observed in both cases, indicative of formation of relatively small amounts of Rh(CO)<sub>2</sub> (14, 18). It is observed that the intensities of all of these features due to (HCO)<sub>2</sub> adsorption are below those observed for CO(g) adsorption. Subsequent CO exposure of the (HCO)<sub>2</sub>-exposed Rh/Al<sub>2</sub>O<sub>3</sub> sample at 300 K causes full development of the expected features due to CO(ads) as shown in Fig. 6e. Thus, exposure to a large dose of (HCO)<sub>2</sub>(g) does not cause full occupancy of all Rh sites capable of CO adsorption. Similar behavior was also observed with the H<sub>2</sub>CO adsorbate.

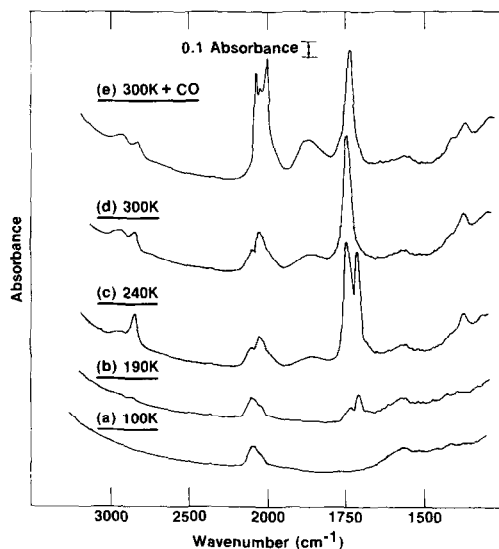


FIG. 6. Infrared spectrum of (HCO)<sub>2</sub> chemisorbed on Rh/Al<sub>2</sub>O<sub>3</sub>.

### V. INTERACTION OF MOLECULAR AND ATOMIC HYDROGEN WITH CO ADSORBED ON Rh—RESULTS

In earlier work, the exposure of dispersed Rh on  $\text{Al}_2\text{O}_3$  to a mixture of  $\text{H}_2(\text{g})$  and  $\text{CO}(\text{g})$  at 300 K resulted in infrared spectra comparable to that obtained for pure CO exposures (21). In addition, LEED studies and thermal desorption studies have indicated that repulsive  $\text{CO}(\text{ads})\text{--H}(\text{ads})$  interactions occur on Rh(111), leading to a lowering of the desorption energy for  $\text{H}(\text{ads})$  (22). Thus it might be expected that the competition between  $\text{H}_2(\text{g})$  and  $\text{CO}(\text{g})$  for Rh adsorption sites would favor CO if the temperature is sufficiently high, permitting rapid  $\text{H}_2$  desorption following addition of CO.

In Fig. 7, a 2.2% Rh/ $\text{Al}_2\text{O}_3$  sample was first saturated at 310 K with CO, giving the infrared spectrum 7a, which is typical for pure CO adsorption (14, 15, 18, 21). The CO was pumped away and the CO-saturated sample was exposed to  $\text{D}_2(\text{g})$  at 102 Torr and 310 K. Following 19 h exposure spectrum 7b was obtained. There is some

loss of intensity at  $2101\text{ cm}^{-1}$  and at  $2031\text{ cm}^{-1}$  corresponding to a decrease in the concentration of  $\text{Rh}(\text{CO})_2$  species. Similar effects have been observed during reversible thermal desorption of CO from these surfaces (14). In addition, slight exchange of  $\text{Al}_2\text{O}_3$ -bound hydrogen, ( $\text{AlOH}$ ), with deuterium is observed by the appearance of enhanced intensity in a broad band with its peak maximum at  $2650\text{ cm}^{-1}$ . This deuterium exchange at 310 K occurs only with the involvement of Rh sites for chemisorptive  $\text{D}_2$  dissociation followed by D migration on the  $\text{Al}_2\text{O}_3$  and has been studied previously (23). An additional exposure to  $\text{D}_2(\text{g})$  at 282 Torr resulted in only slight changes in intensity but yielded no additional infrared features. The cell was then evacuated,  $\text{CO}(\text{g})$  was added to resaturate the Rh surface, and the CO was then evacuated while cooling to 90 K. The cell was then filled with 0.1 Torr of  $\text{D}_2(\text{g})$  and the tungsten atomization filament was turned on to bombard the surface with atomic D. A substantial drop in  $\text{D}_2(\text{g})$  pressure occurred, and the substrate temperature increased to 170 K. Infrared spectra corresponding to various amounts of atomic D bombardment of the surface are shown in Figs. 7c and d. A total exposure to  $\sim 2 \times 10^{19}$  D atoms corresponds to spectrum 7d. No new spectral features were observed during this treatment.

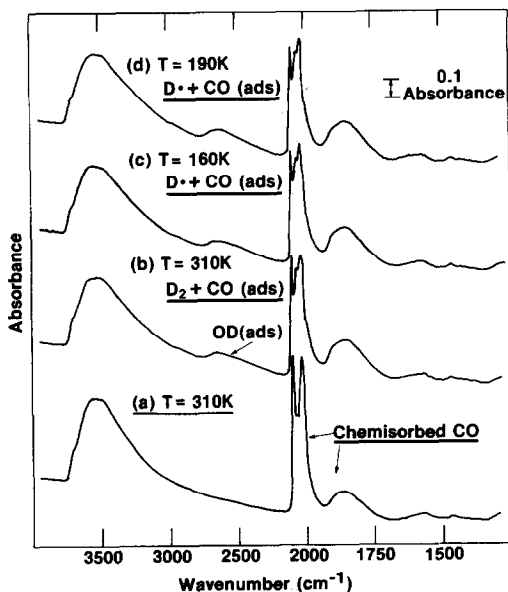


FIG. 7. Interaction of atomic deuterium with chemisorbed CO on Rh/ $\text{Al}_2\text{O}_3$ .

### VI. DISCUSSION

#### A. The Infrared Spectrum of the HCO Ligand

Using matrix isolation techniques, the infrared spectrum of HCO has been measured in a CO matrix at 14–20 K (24, 25). It exhibits a  $\text{C}=\text{O}$  stretching mode at  $1860\text{ cm}^{-1}$ , an intense  $\text{C}\text{--H}$  stretching mode at  $2488\text{ cm}^{-1}$  (25), and a  $\text{H}\text{--C}=\text{O}$  bending vibration at  $1090\text{ cm}^{-1}$  (24, 25). HCO is characterized by a weak  $\text{C}\text{--H}$  bond and by a corresponding high  $\text{C}=\text{O}$  stretching frequency (25, 26). Synthesis of matrix-isolated HCO is achieved at low temperatures



by the interaction of energetic (photolytically produced) H atoms with a CO matrix. In attempts to use thermalized H atoms reacting with CO in an Ar matrix, no reaction has been observed (27).

When HCO is bound as a ligand to transition metal atoms, the C=O stretching frequency is usually observed to shift downwards to  $1600\text{ cm}^{-1}$  and an increase of  $100\text{--}200\text{ cm}^{-1}$  in the CH stretching frequency is observed. A summary of information regarding characteristic frequencies for the HCO moiety is given in Table 2.

On the basis of Table 2 it would seem appropriate to search for HCO(ads) infrared features in the range  $1500\text{--}1800\text{ cm}^{-1}$  ( $\nu_{\text{C-O}}$ ) and in the range  $2500\text{--}2700\text{ cm}^{-1}$  ( $\nu_{\text{H-C}}$ ). The bending vibration below  $1100\text{ cm}^{-1}$  is in an experimentally difficult region in this work due to strong absorption by the  $\text{Al}_2\text{O}_3$  support.

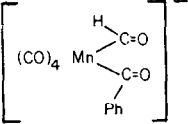
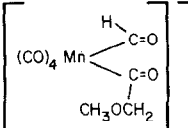
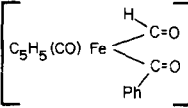
### B. Lack of Evidence for Production of HCO(ads) from Either $\text{H}_2\text{CO}$ or $(\text{HCO})_2$ on Rh/ $\text{Al}_2\text{O}_3$

By comparison of the infrared spectra (Figs. 2 and 3) for  $\text{H}_2\text{CO}$  on  $\text{Al}_2\text{O}_3$  and on Rh/ $\text{Al}_2\text{O}_3$ , it is evident that under no condition of temperature utilized here is there evidence for additional absorption bands on the Rh/ $\text{Al}_2\text{O}_3$  surface in either the region  $1500\text{--}1800\text{ cm}^{-1}$  or the region  $2500\text{--}2700\text{ cm}^{-1}$ . On this basis we can be confident that HCO(ads) is not produced at a spectroscopically detectable level on Rh from  $\text{H}_2\text{CO}$  adsorbate.

The same comparison may be made for  $(\text{HCO})_2$  adsorbate. Here too, no extra absorption bands related to HCO(ads) species on Rh are detected in the region  $1500\text{--}1800\text{ cm}^{-1}$  or the region  $2500\text{--}2700\text{ cm}^{-1}$ . Thus  $(\text{HCO})_2$  is also not a favorable source of

TABLE 2

Infrared Frequencies Observed for the HCO Ligand

Molecule	Wavenumber ( $\text{cm}^{-1}$ )			Ref.
	$\nu_{\text{C-H}}$	$\nu_{\text{C=O}}$	$\nu_{\text{HCO (bend)}}$	
HCO (in CO matrix)	2488	1861	1090	(25)
$\text{Os}(\text{HCO})\text{Cl}(\text{CO})_2(\text{PPh}_3)_2$		1610		(13a)
$[\text{Ir}_4(\text{CO})_{11}(\text{HCO})]^-$		1590–1610		(13b)
		1588		(13c)
		1604		(13c)
		1555		(13c)
$[\text{Et}_4\text{N}][(\text{PhO})_3\text{P}(\text{CO})_3\text{FeHCO}]$		1584		(28)
$[(\text{CO})_4\text{Fe}(\text{CHO})]^-$	2690 2540	1577–1610		(29)

HCO(ads) on an Al<sub>2</sub>O<sub>3</sub>-supported Rh surface.

*C. Atomic Deuterium + CO(ads); Lack of Evidence for DCO(ads) by this Route*

Although expected to be an unlikely route to DCO(ads) formation, a chemisorbed CO layer on Rh was exposed to thermalized D atoms at ~170 K. The D—CO stretching frequency would be expected at about 2000 cm<sup>-1</sup> for DCO(ads). The DC=O stretching frequency would be expected between 1800 and about 1550 cm<sup>-1</sup> (25) [see also Table 2]. Although the 2000-cm<sup>-1</sup> region is strongly overlapped by chemisorbed CO intensity, there is no evidence in either region for additional absorption due to the formation of DCO(ads) species.

*D. Interaction of H<sub>2</sub>CO and (HCO)<sub>2</sub> with Rh/Al<sub>2</sub>O<sub>3</sub>*

The similarity in the infrared spectra for species produced on Rh from H<sub>2</sub>CO and from (HCO)<sub>2</sub> is evident by comparison of Figs. 3 and 6. On the basis of comparisons with intensities achieved for pure CO adsorption, it is clear that both H<sub>2</sub>CO and (HCO)<sub>2</sub> yield appreciable quantities of both terminal-CO and bridged-CO species. These species are present on the crystalline Rh sites described previously (14, 18). The Rh(CO)<sub>2</sub> species are not strongly populated by exposure to H<sub>2</sub>CO or (HCO)<sub>2</sub>, but may be filled by subsequent CO adsorption. A previous model suggested to explain this lack of production of Rh(CO)<sub>2</sub> from H<sub>2</sub>CO adsorption postulated the formation of H—Rh—CO species from H<sub>2</sub>CO (21). This picture was based on the observation of a *shifted* Rh(CO)<sub>2</sub> doublet when H<sub>2</sub>CO + CO were adsorbed. The work reported here in Section III.C has shown that this shift was in fact due to interaction of the Rh(CO)<sub>2</sub> with adsorbates produced by H<sub>2</sub>CO on the Al<sub>2</sub>O<sub>3</sub> support. We now believe that neither H<sub>2</sub>CO nor (HCO)<sub>2</sub> decomposes appreciably on the isolated Rh sites.

Two factors may be responsible for this low reactivity of the isolated Rh sites:

- (1) both H<sub>2</sub>CO and (HCO)<sub>2</sub> require multiple sites to dissociatively chemisorb,
- (2) the special electronic character of isolated Rh sites prohibits dissociative chemisorption of H<sub>2</sub>CO and (HCO)<sub>2</sub>. There is evidence that the isolated sites are in fact Rh<sup>+</sup> species (18). Primet and Garbowski have assigned these sites as Rh(I) based on uv-visible diffuse-reflectance spectral studies of a Rh—Na zeolite (30).

*E. Interaction of H<sub>2</sub>CO with Al<sub>2</sub>O<sub>3</sub>*

Upon warming the H<sub>2</sub>CO/Al<sub>2</sub>O<sub>3</sub> sample from 100 to 300 K, several distinct transitions occur. By 160 K, the intensity of the 3730- and 3660-cm<sup>-1</sup> features due to free OH on Al<sub>2</sub>O<sub>3</sub> was decreased by a factor of 2, while the broad hydrogen-bonded OH feature near 3500 cm<sup>-1</sup> has increased in intensity significantly. Previous work on silica surfaces (31, 32) has shown that free-OH features can be shifted by as much as 350 cm<sup>-1</sup> to lower wavenumber due to interaction with R<sub>2</sub>CO groups. We therefore suggest that at 160 K, evidence for a site-specific interaction of H<sub>2</sub>CO on Al<sub>2</sub>O<sub>3</sub> exists.

Simultaneously, distinct features appear at lower wavenumber which indicate the presence of molecularly adsorbed H<sub>2</sub>CO (see Table 3). The observed shifts and/or multiple peaks observed for  $\nu_5$ ,  $\nu_4$ ,  $\nu_3$ , and  $\nu_2$  could be attributed to either

- (a) a single binding site on Al<sub>2</sub>O<sub>3</sub> which reduces the symmetry of the adsorbed species from the gas-phase symmetry of C<sub>2v</sub>, or
- (b) adsorption at a number of distinct binding sites.

Additional warming serves to clarify the situation. Once the sample has reached room temperature, all of the features observed at 200 K (with the exception of the 1470-cm<sup>-1</sup> feature) have maximized in strength, and have begun to diminish. Three new features have also become apparent, dominating Fig. 2e at 1392, 1372,

TABLE 3

Infrared Features for H<sub>2</sub>CO

Mode	Gas phase <sup>a</sup>	Al <sub>2</sub> O <sub>3</sub> (<200 K)
2ν <sub>3</sub>	2973	2974
ν <sub>4</sub> <i>asym</i> C—H stretch	2874	2910
ν <sub>1</sub> <i>sym</i> C—H stretch	2780	2785
2ν <sub>6</sub>	2081	2040
ν <sub>2</sub> C=O stretch	1743.6	1700
ν <sub>3</sub> CH <sub>2</sub> scissors	1503	1470 1433 1395
ν <sub>5</sub> CH <sub>2</sub> rock	1280	1280 1230
ν <sub>6</sub> CH <sub>2</sub> wag	1167	1150

<sup>a</sup> Ref. (33).

and 1594 cm<sup>-1</sup>. Greenler (17a) has attributed these modes to formate (HCOO) formation from CH<sub>3</sub>OH decomposition on Al<sub>2</sub>O<sub>3</sub>. Evacuation of the sample further reduces the intensity above 1700 cm<sup>-1</sup> and below 1350 cm<sup>-1</sup>. In most of the spectral regions of interest, it is not possible to make a meaningful measure of the loss of intensity, since formate modes and formaldehyde modes will be unresolved. For instance, in the C—H stretching region, as the conversion of H<sub>2</sub>CO to formate occurs, the contributions from the formate C—H stretch (17b) would be expected to compensate for loss of formaldehyde C—H stretch absorption. However, the CH<sub>2</sub> deformation mode observed at 1470 cm<sup>-1</sup> is spectrally isolated from any formate modes. This feature neither shifts nor changes in intensity after the sample has reached 200 K. This clearly indicates the presence of a site which is stable for formaldehyde bonding between 200 and 310 K. Thus, at least two sites exist for the binding of H<sub>2</sub>CO to Al<sub>2</sub>O<sub>3</sub>. One site associated with the CH<sub>2</sub> mode at 1470 cm<sup>-1</sup>, and another site on which formaldehyde converts to formate.

### F. Interaction of (HCO)<sub>2</sub> with Al<sub>2</sub>O<sub>3</sub>

In the process of carrying out the control experiments with (HCO)<sub>2</sub> on Al<sub>2</sub>O<sub>3</sub>, an interesting temperature dependence was observed in the infrared spectra, as shown in Fig. 5. At temperatures below ~250 K, the dominant carbonyl stretching feature is seen at 1720 cm<sup>-1</sup>; upon warming above 250 K, the 1720-cm<sup>-1</sup> feature disappears and a 1748-cm<sup>-1</sup> feature is enhanced. The species corresponding to the 1748-cm<sup>-1</sup> feature is involatile at 305 K as shown in spectrum 5e.

We assign the 1720-cm<sup>-1</sup> feature to monomeric (HCO)<sub>2</sub> adsorbed on Al<sub>2</sub>O<sub>3</sub>. For comparison (HCO)<sub>2</sub>(g) exhibits a fundamental ν<sub>CO</sub> of 1745 cm<sup>-1</sup> (34). (HCO)<sub>2</sub> may exist as a *cis* or *trans* isomer, but both isomers have been shown to exhibit a ν<sub>CO</sub> within 1 cm<sup>-1</sup> of each other. Thus, the adsorption by Al<sub>2</sub>O<sub>3</sub> of (HCO)<sub>2</sub> monomer is associated with a 25-cm<sup>-1</sup> decrease in ν<sub>CO</sub>, compared to (HCO)<sub>2</sub>(g). In this context, we have observed that *physisorbed* <sup>13</sup>CO on Al<sub>2</sub>O<sub>3</sub> at 100 K produces an absorption band at 2190 cm<sup>-1</sup>, or a shift to *higher* wavenumber of 13 cm<sup>-1</sup> from the gas value. This suggests that the monomer (HCO)<sub>2</sub>(ads) is rather strongly perturbed electronically in its adsorptive interaction with Al<sub>2</sub>O<sub>3</sub>.

The 1748-cm<sup>-1</sup> feature which forms extensively above ~250 K is assigned as a polymer of (HCO)<sub>2</sub>. It is well known that (HCO)<sub>2</sub> will polymerize easily and Harris (34) has published an infrared spectrum of the polymer which coated his gas cell windows during ir studies of (HCO)<sub>2</sub>(g). Careful measurement of the literature spectrum indicates that ν<sub>CO</sub> for this polymer was observed at 1747 cm<sup>-1</sup>, in good agreement with our feature on Al<sub>2</sub>O<sub>3</sub> at 1748 cm<sup>-1</sup>.

Features in the C—H stretching region at 2930 and 2840 cm<sup>-1</sup> are assigned as polymer and monomer species, respectively, and on warming their relative intensity changes roughly parallel the ν<sub>CO</sub> intensity changes. (HCO)<sub>2</sub>(g) exhibits ν<sub>CH</sub> = 2844 cm<sup>-1</sup> (34), in good agreement with this assignment,

whereas the condensed polymer exhibits a weak C-H stretching mode at  $2924\text{ cm}^{-1}$  (34).

#### VII. SUMMARY

(1) The adsorption of  $\text{H}_2\text{CO}$  or  $(\text{HCO})_2$  on  $\text{Rh}/\text{Al}_2\text{O}_3$  surfaces produces species having similar infrared spectra in the carbonyl stretching region. These species resemble chemisorbed CO at low coverages on crystalline Rh sites. However the  $\text{Rh}(\text{CO})_2$  species observed for CO adsorption on isolated Rh(I) sites are not readily produced from either  $\text{H}_2\text{CO}$  or  $(\text{HCO})_2$ .

(2) No spectral evidence at  $T \geq 100\text{ K}$  is found for the stabilization of chemisorbed HCO (or DCO) species on  $\text{Al}_2\text{O}_3$ -supported Rh when  $\text{H}_2\text{CO}$ ,  $(\text{HCO})_2$ , or atomic D + CO(ads) are used as potential sources of chemisorbed HCO (or DCO).

(3) Stable surface species are produced from the interaction of  $\text{H}_2\text{CO}$  or  $(\text{HCO})_2$  with  $\text{Al}_2\text{O}_3$ .

We conclude that quantities of HCO(ads) species cannot be stabilized by chemisorption on Rh surfaces or on Rh(I) sites present on  $\text{Al}_2\text{O}_3$ -supported Rh, even at low temperatures. This observation suggests that mechanisms involving adsorbed hydrogen atom attack on chemisorbed CO to eventually produce hydrocarbon products may be unrealistic.

#### ACKNOWLEDGMENTS

The authors would like to thank Drs. S. M. Girvin and T. M. Duncan for many profitable discussions. This work is partially supported by the Office of Naval Research, Contract N0001478F0008.

#### REFERENCES

- (a) Goodman, D. W., Kelley, R. D., Madey, T. E., and Yates, J. T., Jr., *J. Catal.* **63**, 226 (1980). (Also see earlier references therein to work on supported Ni which originally suggested a dissociative CO mechanism.) (b) For a recent review, see Ponoc, V., *Catal. Rev. Sci. Eng.* **18**, 151 (1978).
- Ekerdt, J. G., and Bell, A. T., *J. Catal.* **58**, 170 (1979).
- Rabo, J. A., Risch, A. P., and Poutsma, J. L., *J. Catal.* **53**, 295 (1978).
- Della Betta, R. A., and Shelef, M., *J. Catal.* **48**, 111 (1977); see also *J. Catal.* **60**, 169 (1979).
- Sexton, B. A., and Somorjai, G. A., *J. Catal.* **46**, 167 (1977).
- Castner, D. G., and Somorjai, G. A., *Surf. Sci.* **83**, 60 (1979).
- Yates, J. T., Jr., Williams, E. D., and Weinberg, W. H., *Surf. Sci.* **91**, 562 (1980); see also Castner, D. G., Dubois, L. H., Sexton, B. A., and Somorjai, G. A., *Surf. Sci.* **103**, L134 (1981); Yates, J. T., Williams, E. D., and Weinberg, W. H. *Surf. Sci.* to be published.
- Muettterties, E. L., and Stein, J., *Chem. Rev.* **79**, 479 (1979).
- Mills, G. A., and Steffgen, F. W., *Catal. Rev.* **8**(2), 159 (1973).
- Goodman, D. W., Madey, T. E., Ono, M., and Yates, J. T., Jr., *J. Catal.* **50**, 279 (1977).
- Yates, J. T., Jr., Madey, T. E., and Dresser, M. J., *J. Catal.* **30**, 260 (1973).
- Worley, S. D., and Yates, J. T., Jr., *J. Catal.* **48**, 395 (1977).
- (a) Collins, T. J., and Roper, W. R., *J. Chem. Soc. Chem. Commun.*, 1044 (1976). (b) Pruett, R. L., Schoening, R. C., Vidal, J. L., and Fiato, R. A., *J. Organomet. Chem.* **182**, C57 (1979). (c) Gladysz, J. A., and Selover, J. C., *Tetrahedron Lett.* **4**, 319 (1978).
- Yates, J. T., Jr., Duncan, T. M., Worley, S. D., and Vaughan, R. W., *J. Chem. Phys.* **70**, 1219 (1979).
- Cavanagh, R. R., and Yates, J. T., Jr., *J. Chem. Phys.* **75**, 1551 (1981).
- Norrish, R. G. W., and Griffiths, G. A., *J. Chem. Soc.*, 2829 (1928).
- (a) Greenler, R. G., *J. Chem. Phys.* **37**, 2094 (1962); (b) Donaldson, J. D., Knifton, J. F., and Ross, S. D., *Spectrochim. Acta* **20**, 847 (1964); (c) Noto, Y., Fukuda, K., Onishi, T., and Tamaru, K., *Trans. Faraday Soc.* **63**, 2300 (1967); (d) Ito, M., and Syetake, W., *J. Phys. Chem.* **79**, 1190 (1975).
- Cavanagh, R. R., and Yates, J. T., Jr., *J. Chem. Phys.* **74**, 4150 (1981).
- Thiel, P. A., Williams, E. D., Yates, J. T., Jr., and Weinberg, W. H., *Surf. Sci.* **84**, 199 (1979).
- Dubois, L. H., and Somorjai, G. A., *Surf. Sci.* **91**, 514 (1980).
- Yates, J. T., Jr., Worley, S. D., Duncan, T. M., and Vaughan, R. W., *J. Chem. Phys.* **70**, 1225 (1979).
- Williams, E. D., Thiel, P. A., Weinberg, W. H., and Yates, J. T., Jr., *J. Chem. Phys.* **72**, 3496 (1980).
- Cavanagh, R. R., and Yates, J. T., Jr., *J. Catal.* **68**, 22 (1981).
- Ewing, G. E., Thompson, W. E., and Pimentel, G. C., *J. Chem. Phys.* **32**, 927 (1960).

25. Milligan, D. E., and Jacox, M. E., *J. Chem. Phys.* **41**, 3032 (1964).
26. Adrian, F. J., Cochran, E. D., and Bowers, V. A., *J. Chem. Phys.* **36**, 1661 (1962).
27. Milligan, D. E., and Jacox, M. E., *J. Chem. Phys.* **38**, 2627 (1963).
28. Casey, C. P., and Neumann, S. M., *J. Amer. Chem. Soc.* **98**, 5395 (1976).
29. Collman, J. P., and Winter, S. R., *J. Amer. Chem. Soc.* **95**, 4089 (1973).
30. Primet, M., and Garbowski, E., *Chem. Phys. Lett.* **72**, 472 (1980).
31. Sidorov, A. N., *Zh. Fiz. Khim.* **30**, 995 (1956).
32. Davydov, V. Ya., Kiselev, A. V., and Kuznetsov, B. D., *Zh. Fiz. Khim.* **39**, 2058 (1965).
33. Herzberg, G., "Molecular Spectra and Molecular Structure. II. Infrared and Raman Spectra of Polyatomic Molecules." Van Nostrand-Reinhold, New York, 1945.
34. Harris, R. K., *Spectrochim. Acta* **20**, 1129 (1964).